

# Synthesis and Characterization of Cesium Salt of 12-Tungstophosphoric Acid Supported on SBA-15

Elif Akbay, Gülberk Demir

**Abstract:** 12-tungstophosphoric acid of cesium salt supported on SBA-15 (Cs-TPA/SBA-15) was synthesized by the two-step impregnation technique. Acidic cesium salts supported on SBA-15 at 20%, 40% and 60% loading were synthesized and characterized. Then obtained catalyst have been characterized by XRD, FT-IR, FT-IR spectroscopy of pyridine adsorption, BET analysis, SEM and XRF. It was seen that Cs-TPA was hold on to SBA-15. At high loading percentage, structure of SBA-15 has been deformed.

**Keywords:** 12-Tungstophosphoric Acid Cesium Salt, SBA-15.

## I. INTRODUCTION

Heteropoly acids have strong Brönsted acidity, approaching the super acid sites; HPA on the other hand; are efficient oxidizers exhibiting fast reversible multielectron redox transformations under moderate conditions. Heteropoly acids are known as active catalysts for both homogeneous and heterogeneous acid-catalyzed reactions[1]. They are used in large-scale catalytic processes. Heteropoly acids (HPA) are an alternative to traditional acid catalysts due to their simple preparation, strong acidity and environmental friendliness. Salts of HPA were prepared by partially exchanging protons of the parent HPA with large cations, such as  $\text{Cs}^+$ ,  $\text{K}^+$ ,  $\text{Rb}^+$  and  $\text{NH}_4^+$ , which could be water-insoluble and present a rather high surface area ( $>100 \text{ m}^2/\text{g}$ ). One of the HPA salts is the acidic cesium salt used in this study,  $\text{Cs}_{2.5}\text{H}_{0.5}\text{PW}_{12}\text{O}_{40}$ . This salt has a high surface area and thus a large amount of surface acid sites. Acidic cesium salt,  $\text{Cs}_{2.5}\text{H}_{0.5}\text{PW}_{12}\text{O}_{40}$ , has a high catalytic activity for various acid-catalyzed reactions. This excellent catalysis of  $\text{Cs}_{2.5}\text{H}_{0.5}\text{PW}_{12}\text{O}_{40}$  is attributed to the strong acidity, hydrophobicity, unique pore structure, etc. [2]. In addition, this salt is insoluble in water and polar solvents and has strong acidity. Many reactions are efficiently catalyzed by  $\text{Cs}_{2.5}\text{H}_{0.5}\text{PW}_{12}\text{O}_{40}$  in solid-liquid reaction systems[3]. As pure heteropoly acids have some drawbacks of low surface area, relatively low thermal stability and high solubility in water and polar solvents, they are usually impregnated on different porous materials with high surface area[4]. On the other hand, water-insoluble salts with large monovalent cations such as  $\text{NH}_4^+$ ,  $\text{K}^+$ ,  $\text{Cs}^+$ , have a hard microporous/mesoporous structure and surface area above  $100 \text{ m}^2 \text{ g}^{-1}$ .

Revised Version Manuscript Received on November 13, 2017.

Elif Akbay, Department of Chemical Engineering, Anadolu University, Eskişehir, Turkey.

Gülberk Demir, Department of Chemical Engineering, Anadolu University, Eskişehir, Turkey.

In the other study[5], have studied the catalytic activity, acidity, micro-pore structure of Cs salts. The results attained in this study show that acidic cesium salts ( $\text{Cs}_x\text{H}_{3-x}\text{PW}_{12}\text{O}_{40}$ ) can be controlled with Cs ratios of pore size. Heteropoly acids are supported on different solid materials to overcome obstacles such as low surface area and low thermal [6]. Another disadvantage is that solid heteropolyacids must be deactivated due to coke formation on the catalyst surface during organic reactions. Regular mesoporous materials among various support materials, have been shown to improve the catalytic performance of heteropoly acids.

## II. EXPERIMENTAL

### 2.1. Materials

Tetraethyl orthosilicate (TEOS), Pluronic-123 (triblock copolymer,  $\text{EO}_{20}\text{PO}_{70}\text{EO}_{20}$ ), ethanolamine (EA),  $\text{CS}(\text{NH}_2)_2$ ,  $\text{Pb}(\text{AC})_2$  were obtained from Sigma Aldrich. Ammonium hydroxide and HCl (37%) were supply form Riedel-de Haen.

### 2.2. Preparation of Cs-TPA/SBA-15

SBA-15 was produced by adding 9 ml of tetraethyl orthosilicate (TEOS) to 125 ml of 2 M HCl solution containing 4 g of Pluronic-123. The mixture was stirred for 24 h at  $35^\circ\text{C}$  and permitted to further react at  $100^\circ\text{C}$  overnight in Teflon bottles. The solid product was filtered and washed with deionized water to remove excess HCl. Drying was done at  $30^\circ\text{C}$  and calcination was performed at  $600^\circ\text{C}$  under air flow for 5.5 hours.

Cs-TPA was loaded into the SBA-15 support by the two-step impregnation method. In the first step, the aqueous solution of cesium carbonate was prepared. 1 g of SBA-15 was added to the solution and the product was dried at  $110^\circ\text{C}$  for 2 hours. It was then calcined at  $500^\circ\text{C}$  for 2 hours. In the second step, the solid obtained from the first step was added to the prepared HPA solution. Dried at  $110^\circ\text{C}$  for 2 hours and calcined at  $300^\circ\text{C}$  for 2 hours. Then the sample was stirred for 2 hours in excess of methanol (to separate the free TPA) and 30 min at 12000 rpm, centrifuged and dried overnight at  $100^\circ\text{C}$ .

### 2.3. Characterization of Cs-TPA-SBA-15

The crystallinity and the phase purity of synthesized samples were analyzed by XRD patterns using X-ray diffractometer (Rigaku Rind 2000, Japan). FT-IR studies of the catalysts were conducted by using a Bruker IFS-66.

# Synthesis and Characterization of Cesium Salt of 12-Tungstophosphoric Acid Supported on SBA-15

Lewis and Brønsted acid sites present on the surface of the catalyst were determined with FT-IR spectra of adsorbed pyridine. N<sub>2</sub> adsorption–desorption isotherm measured at 77 K in an automatic adsorption apparatus (ASAP2020; micromeritics). Scanning electron microscopy (SEM) results were obtained on the Zeiss Supra 50 VP Microscope with 20 kV accelerating voltages. X-ray fluorescence (XRF) analysis was carried out by using Rigaku ZSX Primus II.

## III. RESULTS AND DISCUSSION

The synthesized samples have been characterized by using low-angle and wide-angle XRD patterns shown in Figure 1

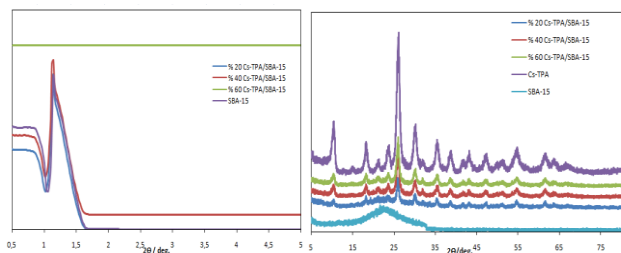


**Figure 1.** a) Low and b) Wide angle XRD diagrams of samples

Figure 1a shows that a very strong peak at  $2\theta=1.5^\circ$  is characteristic peaks of for %20 and %40 Cs-TPA/SBA-15, indicating that they keep the mesoporous structure well. But the peaks are not appearing for 60%Cs-TPA/SBA-15 because there may be chemical interactions between support SBA-15 and Cs-TPA and SBA-15 not keep the mesoporous structure. As seen in Figure 1b, the very broad XRD reflection peak of pure SBA-15 at  $24^\circ$  represents the diffraction of the amorphous wall of SBA-15. Characteristic peaks of Cs-TPA are observed for the all loading in SBA-15, indicating crystallites of Cs-TPA existing on the surface of SBA-15.

All samples were characterized by using FT-IR to investigate the structure of catalysts. The results are shown in Figure 2

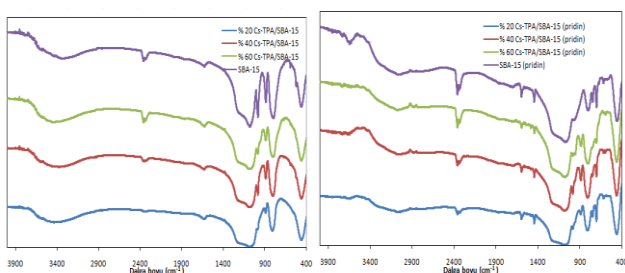


**Figure 2.** a) FT-IR spectra and b) FT-IR (pyridine) spectra of samples

Figure 2a and b shows that the characteristic IR vibration frequencies of the Keggin units and pyridine adsorption are observed for all loading in SBA-15. New adsorption bands appearing in the spectra represent the characteristic of the Brønsted and Lewis acidities at  $1596\text{ cm}^{-1}$  and  $1445\text{ cm}^{-1}$  respectively[6-8].

The surface morphologies of samples were investigated by SEM and the micrographs are presented in Figure 3.

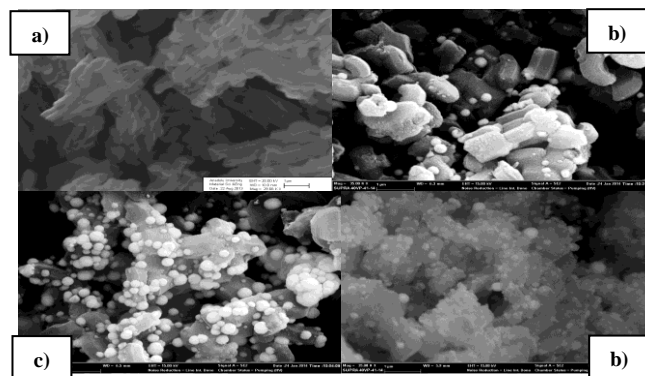


**Figure 3.** SEM spectrum of a)SBA-15 b)% 20 Cs-TPA/SBA-15 c)% 40 Cs-TPA/SBA-15 and d) % 60 Cs-TPA/SBA-15

Images of the SBA-15 denote the formation of rope-like structures with relatively uniform length of about 0.5-8.5  $\mu\text{m}$ . Such a morphology is quite characteristic for SBA-15[9]. As the loading ratio of Cs-TPA to SBA-15 increases, the rope-like structure distorts and length of SBA-15 get shorter. This is observed most intensively at 60% loading, which is also supported by XRD results.

The atomic ratio of W/Cs and the loading % of Cs-TPA nanoparticles inside the SBA-15 were calculated from the XRF analysis, the results are given in Table 1.

**Table 1.** XRF results of Cs-TPA, % 20, % 40, % 60 Cs-TPA/SBA-15

Cs-TPA Loading (%) <sup>a</sup>	Cs <sub>2</sub> O	WO <sub>3</sub>	SiO <sub>2</sub>	W/Cs	Calculated Cs-TPA Loading (%) <sup>a</sup>
20%	2.3987	19.2465	77.0341	4.88	22%
40%	4.5679	36.9688	57.071	4.92	43%
60%	6.5102	54.7042	38.9496	5.1	62%

The composition of determined by XRF analysis of the W/Cs atomic ratio, agreed with the stoichiometric ratio of 4.8, further confirms the formation of crystalline Cs-TPA nanoparticles and the loading % of Cs-TPA nanoparticles inside the SBA-15 for each sample were in acceptable range. N<sub>2</sub> adsorption–desorption isotherms of synthesized samples, calculated by the BJH model from desorption branch, are shown in Figure 4 and the related textual data of the synthesized samples are reported in Table 2.

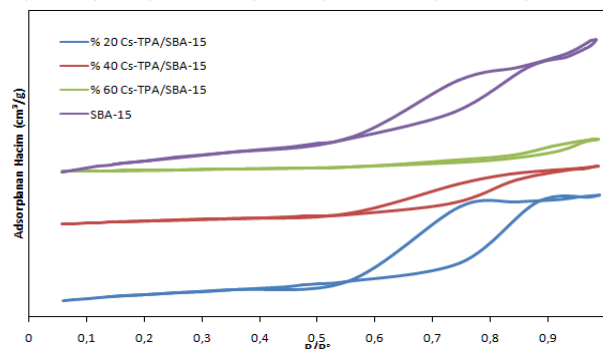


**Figure 4.** N<sub>2</sub> adsorption–desorption isotherms of samples

**Table 2. Surface area, average pore volume and average pore diameter of samples**

	BET Surface	Pore Dia-	Pore Volu-
	Area, (m <sup>2</sup> /g)	Meter, (nm)	me, (cm <sup>3</sup> /g)
SBA-15	511	66.7	0.96
20% Cs-TPA/SBA-15	252	84.5	0.74
40% Cs-TPA/SBA-15	144	89.8	0.41
60% Cs-TPA/SBA-15	65	114.19	0.22

The shape of isotherms for the samples are systematically of type IV according to the IUPAC classification. SBA-15 has a hysteresis loop of H1 type, which is characteristic of cylindrical materials with pores and narrow pore size distribution. The same isotherm type and hysteresis loop were obtained for all loading samples. However, as the Cs-TPA loading % increased, the hysteresis loop became narrower, suggesting a decrease in the pore size of the SBA-15 support. Therefore, SBA-15 maintained its mesostructured morphology, but pore size and pore volumes decreased due to the assembling of Cs-TPA nano particles into the mesoporous SBA-15. As seen in the Table2, upon loading of Cs-TPA into the framework of SBA-15, the surface area and pore volume sharply decrease. This indicates that Cs-TPA particles were assembled within the channels of the SBA-15.

#### IV. CONCLUSIONS

Cs-TPA nanoparticles were loaded on the SBA-15 by the sonochemical method. The synthesized samples were characterized by XRF, XRD, FTIR (pyridine), SEM and N<sub>2</sub> adsorption isotherms. Characterization results show that SBA-15 mesoporous structures conserved their morphology and Cs-TPA nanoparticles were assembled inside the SBA-15 with confirmed loading % and Cs/W ratio of 4.9. In addition, FTIR (pyridine) analysis results confirmed that all samples have Lewis and Brønsted acidity. It was clear that increasing the Cs-TPA loading % resulted in a substantial decrease in the surface area, pore diameter, and pore volume of Cs-TPA-SBA-15 samples. SEM images show that the Cs-TPA nanoparticles were highly dispersed inside the channels of SBA-15 for all loadings. However, as Cs-TPA loading % increased to 60, additional Cs-TPA particles aggregation on the SBA-15 surface was observed as well.

#### REFERENCES

- Okuhara, T., Watanabe, H., Nishimura, T., Inumaru, K. ve Misono, M., (2000), Microstructure of Cesium Hydrogen Salts of 12-Tungstophosphoric Acid Relevant to Novel Acid Catalysis, Chem. Mater., 12, 2230-2238.
- Yoshimune, M., Yoshinaga, Y. ve Okuhara, T. (2002), Effect of alkaline metal on microporosity of acidic alkaline salts of 12-tungstophosphoric acid, Microporous and Mesoporous Materials, 51, 165-174.
- Okuhara, T., Nishimura, T. ve Misono, M. (1996), "Novel Microporous Solid Superacids":CsxH3-x PW12O40 (2<x<3), 11 th Int.Congress on

- Catalysis, 40<sup>th</sup> Anniversary, Studies in Surf. Sci.and Cataly., 101, 581-590.
- Kimura, M., Nakato, T. ve Okuhara, T. (1997), Water-tolerant solid acid catalysis of Cs<sub>2.5</sub>H<sub>0.5</sub>PW<sub>12</sub>O<sub>40</sub> for hydrolysis of esters in the presence of excess water, Applied Catalysis A: General, 165, 227-240.
- Chen, X., Xu, Z., Okuhara, T. (1999) Liquid phase esterification of acrylic acid with 1-butanol catalyzed by solid acid catalysts, Appl. Catal. A, 180 (11-2), 261-269
- Mizuno, M. ve Misono, M. (1998), "Heterogeneous Catalysis," Chem. Rev., 98, 199-217.
- Akçay, M. (2004), FT-IR spectroscopic pyridine on the raw sepiolite and Fe-pillared sepiolite from anatolia, J. of Molec. r Struc 694, 21-26.
- Reddy, C. R., Nagendrappa, G., B. S. (2007), " Surface acidity study of Mn-montmorillonite clay catalysts by FT-IR spectroscopy: Correlation with esterification activity," Catalysis Communications, 8, 241-246.
- Thongtem, T., Phuruangrat, (2009) Effect of basicity on the morphologies of ZnO using a sonochemical method, Curr. Appl. Phys. 9: S197